Desalination and Water Treatment
www.deswater.com

doi: 10.5004/dwt.2017.20585

74 (2017) 248–257
May

Novel synthesis of graphene oxide with polystyrene for the adsorption of toluene, ethylbenzene and xylenes from wastewater

Avideh Azizi[a], Ali Torabian[b,*], Elham Moniri[c], Amir Hessam Hassani[a], Homayon Ahmad Panahi[d]

[a]*Department of Environmental Engineering, Faculty of Environment and Energy, Science and Research Branch, Islamic Azad University, Poonak sq. Ashrafi Esfahani Blv., Hesarak, Tehran 14515-775, Iran, emails: avideh_85@yahoo.com (A. Azizi), ahhassani@srbiau.ac.ir (A.H. Hassani)*
[b]*Faculty of Environment, University of Tehran, No. 25, Ghods St., Enghelab Ave., Tehran 14155-6135, Iran, Tel. +98-91-2125-7996; Fax: +98-21-6640-7719, email: atorabi@ut.ac.ir*
[c]*Department of Chemistry, Varamin (Pishva) Branch, Islamic Azad University, Shahrak Naghsh Jahan, Pishva 33817-74895, Iran, email: moniri30003000@yahoo.com*
[d]*Department of Chemistry, Central Tehran Branch, Islamic Azad University, Shahrak Ghods, Simaye Iran, Tehran 14676-86831, Iran, email: h.ahmadpanahi@iauctb.ac.ir*

Received 14 September 2016; Accepted 8 February 2017

ABSTRACT

The main goal of this research was to evaluate the adsorption capacity of toluene, ethylbenzene and *xylenes* (TEX) onto graphene oxide nanoparticles grafted with polystyrene (GO-PS). Graphene oxide was polymerized using ammonium persulfate initiator. The properties of adsorbents were analyzed by Fourier transform infrared resonance spectroscopy, energy-dispersive X-ray spectroscopy, scanning electron microscopy and Brunauer–Emmett–Teller analysis. This paper includes the elements affective adsorption of TEX such as contact time, pH and adsorbent dose. The adsorption capacity was enhanced with the increasing of contact time and adsorbent dose, but changed insignificantly with pH. The findings demonstrated that an optimum TEX removal efficiency was achieved at contact time of 30 min and adsorbent dose of 1 g/L at 20 mg/L initial TEX concentration (solution pH = 7). The different models were applied to predict the mechanisms of adsorption. The isotherm and kinetic models which best displayed the outcome obtained were the Freundlich model and pseudo-second-order kinetic for TEX, respectively. In addition to the main aim of present study, GO-PS was regenerated for nine cycles and the reused adsorbent exhibited the adsorption ability equivalent to the original, approximately.

Keywords: Graphene oxide; Polystyrene; TEX; Isotherm; Kinetic; Regeneration

1. Introduction

In the last few decades, water pollution problem has become acute. One of the most toxic contaminants is the petroleum hydrocarbons due to release of petroleum products, diesel fuel and gasoline from leaking storage tanks [1]. Toluene, ethylbenzene and xylenes (TEX) characterized by benzene rings are used in solvents and exist in chemical and petrochemical industries [2,3]. TEX are known to pose carcinogenic health hazards [4]. Untreated wastewater of these industries may result in adverse effects on human life and environment. Therefore, TEX compounds should be removed from aqueous solutions because of their high toxicity to human health, air, soil and water [3]. Several treatment techniques have been applied for the removal of TEX from environment. Simplicity, low cost, high efficiency and recovery of adsorbent have made the adsorption process preferable among the other conventional techniques for the

* Corresponding author.

removal of these pollutants from aqueous solutions [2,5]. Additionally, adsorption is one of the most effective procedures for decreasing of organic and inorganic contaminants from industries effluent [6].

Carbon-based materials have been applied for adsorption process due to their good chemical stability making them desirable for large-scale application [7]. Graphene is the newest member of carbon family which has attracted attention from many researchers due to its promising physical and chemical properties and its flexible structure [8]. Recently, graphene was applied as adsorbent for the removal of organic and inorganic pollutants [9]. Previous studies proved insignificant change in the adsorption efficiency of graphene after multiple application and reuse [7]. One derivative of graphene is graphene oxide (GO) that consists of graphene sheets with oxygen-containing functional groups [10]. GO can be prepared using various methods. Among these procedures, Hummers method is the most popular, because of a safe and easy making procedure [11]. In addition, functionalization of graphene can improve its dispersion in solvents, facilitating its application [12]. Polymerization of graphene also can enhance its process ability [12].

Therefore, in the present work, GO was synthesized using the method introduced by Hummers and Offeman [13] and then grafted with polystyrene using ammonium persulfate (APS) initiator. Afterwards, graphene oxide nanoparticles grafted with polystyrene (GO-PS) was applied for the removal of TEX from aqueous solution. The effects of contact time, pH and adsorbent dose on the performance of adsorption process were determined. The purpose of this work was not only to present new adsorption data, but also to report the possibility of regenerating and reusability of the adsorbent. Finally, adsorption isotherms at different adsorbent doses were studied and kinetics of adsorption were investigated.

2. Materials and methods

2.1. Materials

The chemicals tested in this study were graphite powder (particle size <50 μm, purity ≥99.5%, Merck, Germany), H_2SO_4 (95%–97%, Merck, Germany), $NaNO_3$ (Merck, Germany), $KMnO_4$ (Merck, Germany), H_2O_2 (30%, Merck, Germany), HCl (37%, Merck, Germany), dimethylformamide (purity ≥99.8%, Merck, Germany), allylamine (purity <99.5%, Fluka, USA), ammonium persulfate (Merck, Germany), NaOH (Merck, Germany), styrene (Chem-Lab, Belgium), methanol (purity ≥99.5%, Merck, Germany), sodium acetate trihydrate (Merck, Germany), acetic acid (acidimetric >99.5%, Merck, Germany), sodium hydrogen phosphate (Merck, Germany), sodium dihydrogen phosphate (Merck, Germany), toluene (purity ≥99%, Merck, Germany), ethylbenzene (purity ≥99%, Merck, Germany) and xylene (purity ≥99.8%, Merck, Germany).

2.2. Synthesis of GO

GO was prepared from graphite powder by the Hummers and Offeman method [13]. In brief, the mixture of H_2SO_4 (230 mL) and $NaNO_3$ (5 g) was added into the 5 L beaker containing 10 g of graphite. Next, 30 g of $KMnO_4$ was slowly added and stirred for 2 h in ice-water bath. The distilled water (460 mL) was added to the suspension. Later, 325 mL of H_2O_2 (30%) was added into the breaker with stirring while the temperature of the dispersion was kept between 90°C and 100°C for 2 h. After filtering, the mixture was washed using HCl (3%) and also with distilled water for several times. The filtered cake was dried at 45°C for 2 d in oven to obtain dark brown GO powder. GO was characterized via Fourier transform infrared spectroscopy (FTIR; Thermo Nicolet, model: NEXUS 870 FT-IR, USA), energy-dispersive X-ray spectroscopy and scanning electron microscopy (EDX and SEM; Zeiss, model: Sigma, Germany) and Brunauer–Emmett–Teller (BET; BELSORP-mini II, Japan) techniques.

2.3. Grafting of GO with polystyrene:

GO solution was prepared by dissolving 2 g of GO in dimethylformamide (20 mL). The solution was stirred at room temperature while 10 mL of allylamine was added to the solution. The mixture was stirred at 160 rpm for 2 d. Thereafter, the suspension was washed with 20 mL of dimethylformamide. The solution was filtered and dried at room temperature. The grafting of GO with allylamine (GO-AA) was analyzed by FTIR spectroscopy. Styrene was washed three times by 5% NaOH to remove the inhibitor and then washed with distilled water. The modified GO was mixed with APS (0.5 g) and methanol (30 mL). The mixture was stirred with magnetic bar. Afterwards, styrene (30 mL) was added to the mixture and the system was then heated at 60°C. The system was fitted with condenser, nitrogen atmosphere and stirred with magnetic bar for 5 h. Finally, the solution was washed with 30 mL of methanol. The mixture was filtered and dried in vacuum oven at 60°C. GO-PS was analyzed using FTIR, EDX, SEM and BET techniques.

2.4. Chemical analysis method

The TEX concentration in water was determined via gas chromatograph (Agilent GC, 6890N) with flame ionization detector (GC-FID) by head space sampling method. The FID test was done the following conditions: temperature of 250°C, makeup of 45 mL/min, air flow at 350 mL/min and H_2 flow of 40 mL/min. A capillary column, HP-5 (length: 30 m, diameter: 0.32 mm, film thickness: 0.25 μm) was employed with N_2 as the carrier gas at a flow rate of 1.7 mL/min. The GC-FID was operated using the injection technique of split (2:1), injector temperature of 210°C and injection volume of 2 μL. The following temperature program was used: 40°C for 3.5 min and 3°C/min to 65°C and then increased to 220°C with the rate of 30°C/min for 1 min.

2.5. Adsorption experiments

A series of 100 mL flasks were placed in a rotary shaker (IKA, KS 260 Basic, Korea) and the solution of TEX with adsorbent was added to the flasks. Next, the mixture was shaken at 150 rpm and filtered with syringe filter. Batch adsorption studies were carried out to investigate the effects of the following parameters: contact time (5, 10, 15, 20, 30 and 60 min), initial pH (4, 5, 6, 7 and 8) and adsorbent dose (0.1, 0.2, 0.5, 1, 2 and 5 g/L) for the removal of TEX from aqueous

solutions using GO-PS at room temperature. Finally, the results of the batch adsorption experiments were determined using GC-FID. The amount of TEX adsorption was calculated using the following equations:

$$q_t = \frac{(C_0 - C_t)v}{m} \quad (1)$$

$$\mathrm{RE}(\%) = \left(\frac{C_0 - C_t}{C_0}\right)100 \quad (2)$$

2.6. Regeneration study of GO-PS

The experiment for the adsorption capacity of the recycled adsorbent was carried out for nine sequential cycles. Adsorbent was washed using methanol and distilled water for every cycle. In this part, GO-PS was regenerated for reusing with the following procedure: 30 min contact time, pH of 7, initial TEX concentration of 20 mg/L, adsorbent dose of 1 g/L, temperature of 23°C and agitation speed of 150 rpm. The suspensions were centrifuged (3,000 rpm for 5 min) and filtered with syringe filter. Finally, the clear supernatant was analyzed by GC-FID.

2.7. Isotherm and kinetic experiments

Isotherms behavior of TEX adsorption on GO-PS was studied using Freundlich, Dubinin–Radushkevich, Temkin and Harkins–Jura models. The Freundlich isotherm can be described for multilayer adsorption on a heterogeneous adsorbent surface (Eq. (3)) [2,14]. The Dubinin–Radushkevich isotherm demonstrates the type of adsorption process basing on chemical or physical mechanism (Eq. (4)) [2,15]. E is the adsorption energy and this value can be described by Eq. (6) [2]. The Temkin isotherm is explained basing on heat of adsorption and the adsorbent–adsorbate interaction on the surface (Eq. (7)) [15]. The Harkins–Jura adsorption model calculates by multilayer adsorption (Eq. (8)) [16]. Isotherm equations of adsorption are shown in Table 1.

In order to interpret the kinetic batch experimental data, four different kinetic models were used: (1) pseudo-first-order model (Eq. (9)) [17], (2) pseudo-second-order model (Eq. (10)) [18], (3) intraparticle diffusion model (Eq. (11)) [2] and (4) Elovich model (Eq. (12)) [17]. The equations of adsorption kinetic are presented in Table 2.

3. Results and discussion

3.1. Characterization

The structure of GO, GO-AA and GO-PS were analyzed by FTIR spectroscopy (Fig. 1). Fig. 1 shows GO characteristic bands, which presents the following functional groups: 1,054 and 1,222 cm^{-1} (C–O stretching vibration), 1,421 cm^{-1} (stretching vibration of CH_2), 1,720 cm^{-1} (C=O groups stretching vibration), and 1,628 and 3,440 cm^{-1} (O–H stretching vibration) [5].

In the spectrum of GO-AA, the C–O peak at 1,034 cm^{-1} is broadened [19]. Adsorption band at 3,363 cm^{-1} which discloses the presence of O–H and N–H groups are of high intensity on GO-AA [20]. For GO-PS, the peak at 1,061 cm^{-1} is assigned to the bond of C–O [21]. Adsorption band of C=C aromatic around wave number 1,552 cm^{-1} is created after grafting GO with polystyrene when compare with GO-AA spectrum [22,23]. Further, the vibration at 2,925 cm^{-1} is observed in GO-PS, which is attributed to –C–H stretching (alkane) [22,23]. Adsorption peak at 3,423 cm^{-1} on GO-PS spectrum confirms the presence of O–H and N–H functional groups [24,25].

The morphology of the prepared materials was investigated using field emission scanning electron microscopy equipped with an EDX detector (Oxford instruments). To understand the elemental composition of the material, the composite was studied using EDX analysis, where, it can be seen that the major elements present are carbon, oxygen and nitrogen. The elemental analysis of GO and GO-PS by EDX is shown in Figs. 2(a) and (b). The weight percentage of C and O calculated from EDX for GO were 57.17% and 42.83% and the percentage of C, O and N for GO-PS reached 45.98%, 46.32% and 7.70%, respectively. The change in the weight percentage for elements was due to the existing nitrogen which confirms good grafting with allylamine and polymerization. The formation of GO-PS is described in Fig. 3.

Table 1
Isotherm equations

Isotherm name	Isotherm equation	Equation	Description
Freundlich	$\log q_e = \log k_f + \frac{1}{n}\log C_e$	(3)	The intercept and slope of the plot of $\log q_e$ vs. $\log C_e$ were used to evaluate k_f and n values
Dubinin–Radushkevich	$\ln q_e = \ln q_m - B\varepsilon^2$	(4)	B can be calculated by the plot of $\ln q_e$ vs. ε^2
	$\varepsilon = \mathrm{RT}\left(1 + \frac{1}{C_e}\right)$	(5)	
	$E = \frac{1}{\sqrt{2B}}$	(6)	
Temkin	$q_e = B_1 \ln k_t + B_1 \ln C_e$	(7)	The values of k_t and B_1 can be obtained by plotting q_e against $\ln C_e$
Harkins–Jura	$\frac{1}{q_e^2} = \frac{B_2}{A} - \frac{1}{A}\log C_e$	(8)	The constants of A and B_2 can be obtained by plotting $1/q_e^2$ against $\log C_e$

Table 2
Kinetic equations

Kinetic name	Kinetic equation	Equation	Description
Pseudo-first-order	$\log q_e - q_t = \log q_e - \frac{k_1}{2.303} t$	(9)	The values of k_1 and q_e can be determined from the slope and intercept of the plotting $\log(q_e - q_t)$ against t
Pseudo-second-order	$\frac{t}{q_t} = \frac{1}{q_e^2 k_2} + \frac{t}{q_e}$	(10)	The values of k_2 and q_e can be evaluated by plotting t/q_t vs. t
Intraparticle diffusion	$q_t = k_p t^{0.5} + c$	(11)	k_p can be calculated from the slope of the plot of q_t vs. $t^{0.5}$
Elovich	$q_t = a - b \ln t$	(12)	The constants a and b can be obtained by plotting q_t against $\ln(t)$

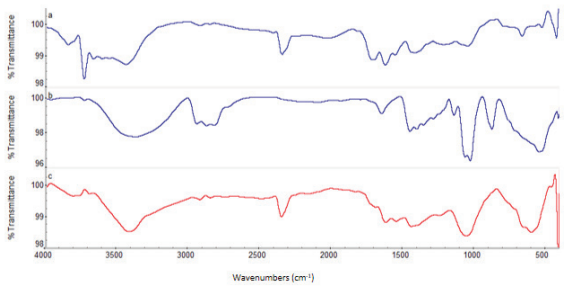

Fig. 1. FTIR spectra of adsorbents: (a) GO, (b) GO-AA and (c) GO-PS.

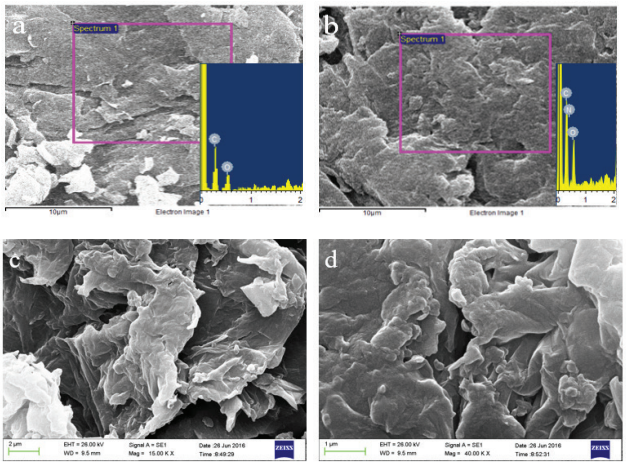

Fig. 2. (a) SEM image and EDX spectrum of GO, (b) SEM image and EDX spectrum of GO-PS, and (c) and (d) SEM images of GO-PS.

The SEM images of GO and GO-PS are illustrated in Fig. 2. The structure of GO consisted of many layers was confirmed by the SEM image (Fig. 2(a)). The image denotes that the GO was synthesized properly. Figs. 2(c) and (d) show the SEM images of porous GO-PS revealing the wrinkles and folds. These crumples show the flexibility of the adsorbent and abundant oxygen-containing functional groups on the sheet of the adsorbent [5].

The BELSORP instrument was used for textural properties of the adsorbents by N_2 adsorption/desorption isotherms

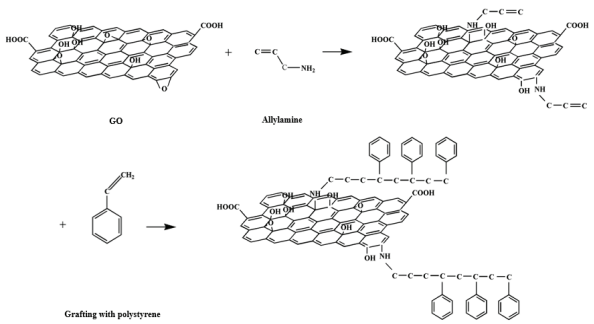

Fig. 3. Representation of the preparation of GO-PS.

at 77 K. The surface area of GO and GO-PS were evaluated by the BET model, while the average pore diameter and total pore volume were estimated with Barrett–Joyner–Halenda theory. The total pore volume was calculated with the adsorbed amount at a relative pressure ($P/P0$) of 0.990. Before grafting of GO, a specific surface area of 13.24 m^2/g, total pore volume of 0.0161 cm^3/g and average pore diameter of 4.853 nm are measured [5]. After polymerization, the surface area, total pore volume and average pore diameter were found to be 9.5262 m^2/g, 0.0168 cm^3/g and 7.0512 nm, respectively. The average pore diameter was increased about twice as the original and total pore volume increased even more. Styrene polymer chains connected to GO takes place between the layers. This phenomenon increases the pore volume diameters. Furthermore, some groups on GO-PS can create space and disperse average pore during aggregation [5,26]. The surface area of the adsorbent decreased with a low amount. The structure of GO-PS is almost similar to GO because polystyrene chains contain phenyl groups that have structure similar to that of the GO. It may be due to the insignificant change in surface area.

3.2. Influence of contact time on TEX adsorption

The effect of contact time on the adsorption of TEX on GO-PS was investigated to determine the equilibrium point. The adsorption experiments were carried out for contact times ranging from 5 to 60 min. The results are shown in Fig. 4. It is observed that, the sharp slope was obtained for TEX adsorption during the first 5 min. The adsorption capacity increased during the second time period (5–30 min) and had no significant change after 30 min. The TEX adsorption achieved

equilibrium in about 30 min. According to these results and our previous work [5], sorbent had good adsorption in the initial stage, which may be due to the high accessibility to the active sites on GO-PS. Similar observations on high adsorption at the beginning of procedure were reported by other researchers [3,5,27–29].

3.3. Influence of pH on TEX adsorption

A pH range of 4–8 was applied for the removal of TEX by GO-PS. The solutions pH of 4 and 5 were adjusted with sodium acetate–acetic acid buffer solutions. The effect of solution pH was investigated in the range between 6 and 8 via adjusting the solution pH with buffer of sodium hydrogen phosphate–sodium dihydrogen phosphate. Fig. 5 depicts the influence of pH on TEX removal. As seen in Fig. 5, increasing the pH range has negligible effect on the adsorption of TEX on GO-PS. These observations are consistent with that of other research [2,30]. According to these results, GO-PS has high stability in the wide ranges of pH.

3.4. Influence of adsorbent dose on TEX adsorption

Other experiments were also carried out to determine the effect of the adsorbent dose on TEX removal in the range of 0.1–5 g/L. The findings are depicted in Fig. 6. It was found that the removal efficiency of TEX increased with increasing the initial amount of GO-PS. The removal efficiency achieved to 60%, 64%, 70% and 70% in 1 g/L of adsorbent for toluene, ethylbenzene, *p*-xylene and *o*-xylene, respectively. At higher dose (5 g/L), the adsorption capacity increased more remarkably. It was found that 79% (toluene), 86% (ethylbenzene), 92% (*p*-xylene) and 90% (*o*-xylene) for every compound. This finding can be explained by the fact that available adsorption sites, the surface area of the adsorbent and active functional groups are enhanced with increasing of adsorbent dose [18,29,31,32]. The optimum point of adsorbent dose was selected as 1 g/L.

The adsorbent preference in the adsorbate is observed in Fig. 6, it decreases in the order of *p*-xylene > *o*-xylene > ethylbenzene > toluene. These results are in agreement with the findings reported by the other researchers for the same compounds [2,4,33]. Toluene had the lowest adsorption capacity among the four compounds because of: (1) high water solubility (toluene = 515 mg/L, ethylbenzene = 152 mg/L, *p*-xylene = 198 mg/L and *o*-xylene = 175 mg/L), (2) low molecular weight (toluene = 92 g/mol, ethylbenzene = 106 g/mol, *p*-xylene = 106 g/mol and *o*-xylene = 106 g/mol) and (3) hydrophobicity (based on their octanol–water coefficient log values) (toluene = 2.69, ethylbenzene = 3.15, *p*-xylene = 3.15 and *o*-xylene = 2.77) [2,4]. Molecular weight of ethylbenzene, *p*-xylene and *o*-xylene is 106 g/mol. Adsorption capacity between the three compounds can be changed meanwhile in this study *p*-xylene had the greatest adsorption. The $-CH_3$ bonds have symmetry that take place on benzene ring in *p*-xylene. The π–π interactions between the rings of adsorbent and *p*-xylene are generated easily because of this symmetry. This can be the reason for that why *p*-xylene has higher adsorption capacity than *o*-xylene and ethylbenzene. Finally, molecular size can also effects the active surface sites available for the adsorption [3,5].

3.5. The regeneration

The recycling and regeneration in sorption processes can help to reuse the used adsorbent reducing the costs of the adsorption [2,34]. GO-PS was washed using methanol and distilled water to regenerate the used adsorbent for nine

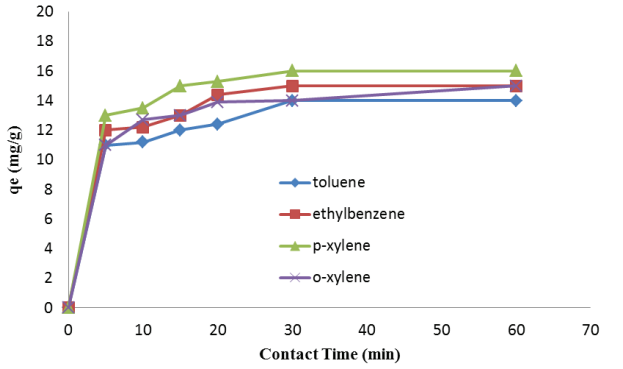

Fig. 4. Effect of contact time on the adsorption of TEX via GO-PS (TEX solution: 20 mg/L; adsorbent dose: 1 g/L; pH: 7; room temperature: 23°C, shaker speed: 150 rpm).

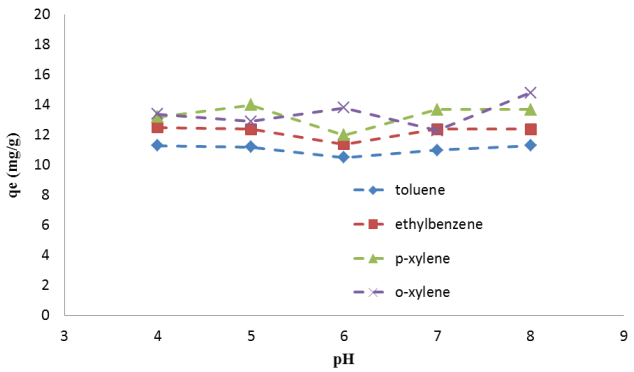

Fig. 5. Effect of pH on the adsorption of TEX by GO-PS (contact time: 30 min; TEX solution: 20 mg/L; adsorbent dose: 1 g/L; room temperature: 23°C, shaker speed: 150 rpm).

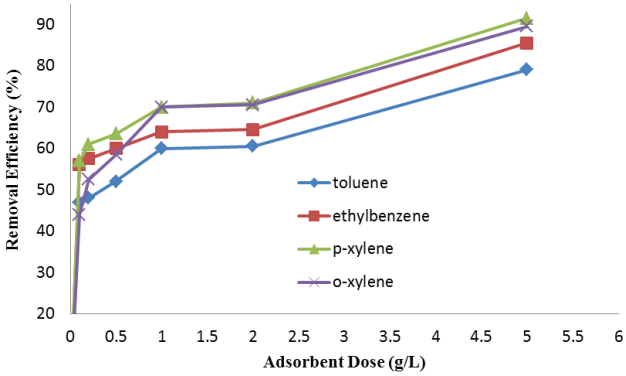

Fig. 6. Effect of adsorbent dose on the TEX removal (contact time: 30 min; TEX solution: 20 mg/L; pH: 7; room temperature: 23°C, shaker speed: 150 rpm).

cycles. The influence of repeated regeneration of GO-PS on the removal efficiency is shown in Fig. 7. At the first regeneration step, a small decrease of 10% is observed in TEX removal amount. Then, the adsorption of GO-PS for TEX was changed negligibly for every compound with increasing of the cycle number. This finding is in agreement with those reported by other researchers [5,7,28,35]. According to these results and our previous work [5], GO-based materials have high ability in the regeneration as an adsorbent, which is likely due to the improvement of the surface and pore volume of the adsorbent during the washing process. Thus, GO-PS can be reused over multiple cycles without any significant loss in its adsorption capacity. It is notable that the TEX adsorbed by the GO-PS could be easily desorbed by washing. Consequently, GO-PS can be used repeatedly in water and wastewater treatment from TEX.

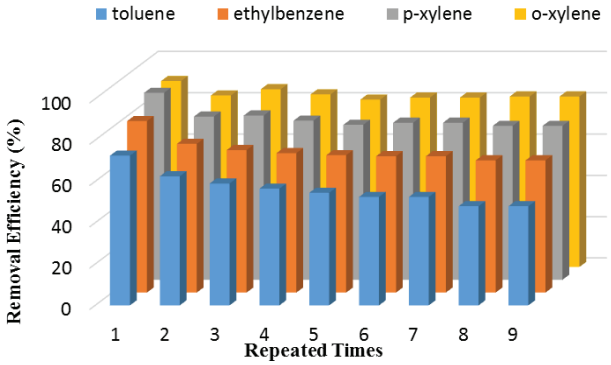

Fig. 7. The regeneration of GO-PS (contact time: 30 min; TEX solution: 20 mg/L; adsorbent dose: 1 g/L; pH: 7; room temperature: 23°C, shaker speed: 150 rpm).

3.6. Isotherm and kinetic studies

3.6.1. Adsorption isotherms

To determine adsorption isotherms, experiments were carried out under the following conditions: contact time = 30 min, initial concentration of TEX = 20 mg/L, pH = 7, agitation speed = 150 rpm and the range of 0.1–2 g/L for the adsorbent dose. Four isotherm models, namely Freundlich, Dubinin–Radushkevich, Temkin and Harkins–Jura were used in the present study.

Isotherms behavior of TEX adsorption on the GO-PS was investigated using models, and the results are presented in Table 3. As seen in Table 3, the Freundlich model fits the experimental data better than the other models with a higher coefficient of determination (R^2) of 0.890, 0.952, 0.947 and 0.933 for toluene, ethylbenzene, *p*-xylene and *o*-xylene, respectively. The Freundlich model demonstrates surface heterogeneity of the adsorbent [18]. The value of E in Dubinin–Radushkevich model shows the type of adsorption process [2]. The adsorption mechanism is physical and chemical in the range of $E < 8$ kJ/mol and $E > 16$ kJ/mol, respectively [2]. Ion-exchange mechanism can be resulted from the range of $8 < E < 16$ kJ/mol [2]. The E parameters shown in Table 3 are from the Dubinin–Radushkevich model, which is in the range of 0.2747–0.5075 kJ/mol. Consequently, influential mechanism is physical adsorption.

3.6.2. Adsorption kinetics

The adsorption kinetics were studied considering the following conditions: initial concentration of TEX = 20 mg/L, pH = 7, the adsorbent dose = 1 g/L, agitation speed = 150 rpm and a range of 5–30 min for contact time. The batch kinetic data were analyzed using pseudo-first-order,

Table 3
Isotherm constants and correlation coefficients for TEX adsorption onto GO-PS

	Toluene	Ethylbenzene	*p*-Xylene	*o*-Xylene
Freundlich				
k_f (L/mg)	2.1923×10^{-6}	1.1371×10^{-9}	1.1068×10^{-4}	2×10^{-2}
n	0.1373	0.0865	0.1565	0.2897
R^2	0.8902	0.9515	0.947	0.933
Dubinin–Radushkevich				
B (mol^2/kJ^2)	4.8752	6.6223	3.175	1.9411
E (kJ/mol)	0.3202	0.2747	0.3968	0.5075
R^2	0.8779	0.945	0.9354	0.9144
Temkin				
k_t (L/mg)	0.1284	0.1408	0.1719	0.1767
B_1	212.98	402.84	235.16	109.86
R^2	0.6928	0.7956	0.8153	0.8651
Harkins–Jura				
A	6.8116	5.3050	11.1358	19.3423
B_2	1.0156	0.9315	0.9053	1.005
R^2	0.6166	0.6075	0.6285	0.5687

pseudo-second-order, intraparticle diffusion and Elovich models.

The constants and R^2 values relevant to the kinetic models are listed in Table 4. Adsorption kinetic data fits better to the pseudo-second-order model than the other models. The R^2 values for pseudo-second-order model were 0.989, 0.994, 0.998 and 0.999 for toluene, ethylbenzene, *p*-xylene and *o*-xylene, respectively.

The values of q_e (experimental) and q_e (calculated) of the pseudo-first-order and pseudo-second-order models are also listed in Table 4. The q_e values for pseudo-second-order model were 14.903 mg/g (toluene), 16.155 mg/g (ethylbenzene), 16.978 mg/g (*p*-xylene) and 14.881 mg/g (*o*-xylene). Based on these results, the values obtained from this model were close to the experimental values, indicating the suitable accuracy of the pseudo-second-order model.

3.7. Comparative study

Comparisons of the adsorption capacity via different adsorbents in TEX removal are summarized in Table 5. Considering the finding of this study, GO-PS has high potential for TEX adsorption capacity. According to the adsorption capacity of GO and GO-A (graphene oxide nanoparticles modified with 4-aminodiphenylamine) in our previous study [5], GO-PS was better than these adsorbents. This can be because of the phenyl rings in GO and styrene which generate π–π interaction with the rings of TEX compounds. Furthermore, it may be due to the fact that the number of styrene polymer chain was high which increases the adsorption of TEX. The adsorption capacity of TEX appeared with no significant changes in a wide pH range, confirming the good stability of the GO-PS as TEX adsorbents in a wide range of pH. On the other hand, the equilibrium contact time of GO-PS was obtained 30 min indicating more suitable for emergency TEX removal in industrial applications which need rapid adsorption process. It is noteworthy that although GAC and CNT listed in Table 5 show higher adsorption capacity than GO-PS, they required the contact time of 480 and 240 min, respectively (which is significantly greater than that of the GO-PS). In addition, GO-PS was capable to be regenerated for nine cycles with good adsorption capacity. Consequently, GO-PS can be proposed an applicable and efficient adsorbent for TEX removal from aqueous solutions.

4. Conclusions

This study investigated a modification method for GO which was efficient, in order to improve the adsorption capacity of TEX. Adsorption equilibrium time was selected as 30 min throughout this research. This characteristic is suitable for the TEX removal which needs rapid treatment. Furthermore, the effect of initial pH on the adsorption of TEX by GO-PS showed that sorbent has stability in the different ranges of pH. The studies exhibited that GO-PS can be regenerated using methanol and distilled water and reused for at least nine cycles without any notable loss in its adsorption capacity, approximately. This finding demonstrated the ability of GO-PS as a cost-benefit adsorbent. The removal efficiency of toluene, ethylbenzene, *p*-xylene and *o*-xylene at the equilibrium condition (contact time = 30 min, adsorbent dose = 1 g/L and pH = 7) was 70%, 75%, 80% and 70%, respectively. Considering the findings of this research, the adsorption behavior of GO-PS fitted well with the Freundlich isotherm (R^2 in the range 0.890–0.952) and the pseudo-second-order model (R^2 in the range 0.989–0.999). Consequently, GO-PS is a new modification of GO that grafted with polystyrene. Because of reusable property and stability of GO-PS, this adsorbent can be considered as one of the functional choices for TEX removal from aqueous solutions.

Table 4
Kinetic parameters for adsorption of TEX onto GO-PS

	Toluene	Ethylbenzene	*p*-Xylene	*o*-Xylene
$q_{e(\text{experimental})}$ (mg/g)	14	15	16	14
Pseudo-first-order				
k_1 (1/min)	0.0444	0.1034	0.1057	0.2093
$q_{e(\text{calculated})}$ (mg/g)	3.9682	6.4803	5.6689	10.8168
R^2	0.9493	0.7968	0.9386	0.8617
Pseudo-second-order				
k_2 (g/mg min)	0.0229	0.0231	0.0292	0.0377
$q_{e(\text{calculated})}$ (mg/g)	14.9031	16.1550	16.9779	14.8809
R^2	0.9888	0.9937	0.9983	0.9992
Intraparticle diffusion				
k_p (mg/g min$^{1/2}$)	0.9277	1.0304	0.9914	0.9192
c	8.5539	9.3589	10.749	9.3865
R^2	0.9184	0.9157	0.9429	0.8802
Elovich model				
a	7.983	8.6397	9.9141	8.448
b	1.5891	1.7978	1.7846	1.7178
R^2	0.8287	0.8572	0.9395	0.9453

Table 5
Comparisons of q_e via various adsorbents in TEX adsorption

Adsorbents	q_e (mg/g)						Conditions		
	Toluene	Ethylbenzene	*p*-Xylene	*o*-Xylene	Xylenes	C_0 (mg/L)	Contact time	Adsorbent dose (g/L)	Ref.
GO-PS	14	15	16	14	–	20	30 min	1	This study
GO	7.8	9.7	10.2	8.8	–	20	5 min	1	[5]
GO-A	11.3	13.6	14	12.2	–	20	5 min	1	[5]
Granulated zeolite nanoparticles	0.898	0.746	–	–	0.674	20	48 h	5	[36]
Montmorillonite modified with polyethylene glycol	4.18	5.12	–	–	6.00	150	24 h	5	[2]
Smectite organoclay	0.69	0.72	0.75	–	–	29.06 (toluene) 8.58 (ethylbenzene) 8.52 (*p*-xylene)	60 min	20	[3]
Ostrich bone waste-loaded a cationic surfactant	119.5	144.1	137.7	–	–	100	60 min	10	[37]
Activated carbon prepared from date pits	5.0	5.6	–	–	6.2	10	–	1	[38]
CNT	80.1	81.1	147.8	–	–	200	4 h	0.6	[39]
CNTs–3.2% O	99.47	115.63	–	–	–	15–110 (toluene) 10–80 (ethylbenzene)	6 h	0.4	[40]
MWCNT	9.8	9.9	–	–	9.9	10	10 min	1	[41]
SWCNT	9.98	9.98	–	–	9.98	10	10 min	1	[41]
Hybrid CNT	9.95	9.96	–	–	9.96	10	10 min	1	[41]
Nano-Fe	9.8	9.8	–	–	9.98	10	10 min	1	[41]
PAC	40	–	–	–	–	100	18 h	2.5	[42]
GAC	194.1	–	–	–	–	35–442	8 h	1.5	[43]
SWCNT	–	–	77.5	–	–	7–107	24 h	0.357	[44]
SWCNT (HNO_3)	–	–	85.5	–	–	7–107	24 h	0.357	[44]
GAC	221.3	250.65	301.4	–	–	20–200	240 min	0.6	[30]
CNT (NaOCl)	279.81	342.67	413.77	–	–	20–200	240 min	0.6	[30]
SWCNT (NaOCl)	103.2	–	–	–	–	200	24 h	0.025	[45]
CNTs–KOH	87.12	322.05	–	–	–	9–60 (toluene) 11–83 (ethylbenzene)	24 h	0.4	[46]
ACF	85	237	185	–	–	100	–	12.5	[30]
PMO	5.147	–	–	–	–	10	50 min	4	[47]

Note: GO-A – graphene oxide nanoparticles modified with 4-aminodiphenylamine, CNT – carbon nanotube, MWCNT – multi-walled carbon nanotubes, SWCNT – single-walled carbon nanotubes, PAC – powdered activated carbon, GAC – granular activated carbon, ACF – activated carbon fiber and PMO – periodic mesoporous organosilica.

Acknowledgments

We are grateful to the Science and Research Branch, Islamic Azad University (SRBIAU) and Iranian Mineral Processing Research Center (IMPRC) for providing research materials and equipment. In addition, the authors would like to express their gratitude to Mrs. Armineh Azizi (PhD graduate of Amirkabir University of Technology (AUT)), Dr. Elaheh Kowsari (Associate Professor of AUT) and Ehssan Hosseini Koupaie (PhD candidate of the

University of British Colombia) for their consultations during the experiments.

Symbols

q_t — Adsorbent capacity of adsorbate, mg/g
RE (%) — Removal efficiency, %
C_0 — Initial concentration of the adsorbate, mg/L
C_t — Concentration of the adsorbate after a certain period of time, mg/L
m — Mass of adsorbent, g
v — Volume of the solution, L
q_e — Adsorption capacity of the adsorbent at equilibrium, mg/g
C_e — Concentration of adsorbate at equilibrium, mg/L
k_f — Freundlich constant, L/mg
n — A constant related the intensity of adsorption
q_m — Theoretical monolayer saturation capacity, mg/g
B — Constant of the sorption energy, mol^2/kJ^2
ε — Polanyi potential
R — Universal gas constant, 8.314 J/mol K
T — Absolute temperature
E — The adsorption energy, kJ/mol
B_1 — A constant related to the heat of adsorption
k_t — The constant of equilibrium binding, L/mg
A — A constant in Harkins–Jura isotherm
B_2 — A constant in Harkins–Jura isotherm
k_1 — Rate constant of pseudo-first-order adsorption, 1/min
k_2 — Rate constant of pseudo-second-order adsorption, g/mg min
k_p — Rate constant of the intraparticle diffusion kinetic model, mg/g $min^{1/2}$
c — A constant in intraparticle diffusion kinetic
a — A constant in Elovich model
b — A constant in Elovich model

References

[1] R. Hosseinzadeh, R. Tahmasebi, K. Farhadi, A.A. Moosavi-Movahedi, A. Jouyban, J. Badraghi, Novel cationic surfactant ion pair based solid phase microextraction fiber for nano-level analysis of BTEX, Colloids Surf., B, 84 (2011) 13–17.
[2] H. Nourmoradi, M. Nikaeen, M. Khiadani (Hajian), Removal of benzene, toluene, ethylbenzene and xylene (BTEX) from aqueous solutions by montmorillonite modified with nonionic surfactant: equilibrium, kinetic and thermodynamic study, Chem. Eng. J., 191 (2012) 341–348.
[3] M.N. Carvalho, M. da Motta, M. Benachour, D.C.S. Sales, C.A.M. Abreu, Evaluation of BTEX and phenol removal from aqueous solution by multi-solute adsorption onto smectite organoclay, J. Hazard. Mater., 239–240 (2012) 95–101.
[4] M. Aivalioti, D. Pothoulaki, P. Papoulias, E. Gidarakos, Removal of BTEX, MTBE and TAME from aqueous solutions by adsorption onto raw and thermally treated lignite, J. Hazard. Mater., 207–208 (2012) 136–146.
[5] A. Azizi, A. Torabian, E. Moniri, A.H. Hassani, H. Ahmad Panahi, Adsorption performance of modified graphene oxide nanoparticles for the removal of toluene, ethylbenzene and xylenes from aqueous solution, Desal. Wat. Treat., 57 (2016) 28806–28821.
[6] M.T. Yagub, T.K. Sen, S. Afroze, H.M. Ang, Dye and its removal from aqueous solution by adsorption: a review, Adv. Colloid Interface Sci., 209 (2014) 172–184.
[7] S. Chowdhury, R. Balasubramanian, Recent advances in the use of graphene-family nanoadsorbents for removal of toxic pollutants from wastewater, Adv. Colloid Interface Sci., 204 (2014) 35–56.
[8] S.P. Dubey, A.D. Dwivedi, I.C. Kim, M. Sillanpaa, Y.N. Kwon, C. Lee, Synthesis of graphene–carbon sphere hybrid aerogel with silver nanoparticles and its catalytic and adsorption applications, Chem. Eng. J., 244 (2014) 160–167.
[9] P. Ganesan, R. Kamaraj, S. Vasudevan, Application of isotherm, kinetic and thermodynamic models for the adsorption of nitrate ions on graphene from aqueous solution, J. Taiwan Inst. Chem. Eng., 44 (2013) 808–814.
[10] Y. Zhang, L. Yan, W. Xu, X. Guo, L. Cui, L. Gao, Q. Wei, B. Du, Adsorption of Pb(II) and Hg(II) from aqueous solution using magnetic $CoFe_2O_4$-reduced graphene oxide, J. Mol. Liq., 191 (2014) 177–182.
[11] T.T. Wu, J.M. Ting, Preparation and characteristics of graphene oxide and its thin films, Surf. Coat. Technol., 231 (2013) 487–491.
[12] L. Xu, X. Yang, Molecular dynamics simulation of adsorption of pyrene–polyethylene glycol onto graphene, J. Colloid Interface Sci., 418 (2014) 66–73.
[13] W.S. Hummers, R.E. Offeman, Preparation of graphitic oxide, J. Am. Chem. Soc., 80 (1958) 1339.
[14] M. Yuan, S. Tong, S. Zhao, C.Q. Jia, Adsorption of polycyclic aromatic hydrocarbons from water using petroleum coke-derived porous carbon, J. Hazard. Mater., 181 (2010) 1115–1120.
[15] A. Azizi, M.R. Alavi Moghaddam, M. Arami, Performance of pulp and paper sludge for reactive blue 19 dye removal from aqueous solutions: isotherm and kinetic study, J. Residuals Sci. Technol., 7 (2010) 173–179.
[16] N.K. Amin, Removal of direct blue-106 dye from aqueous solution using new activated carbons developed from pomegranate peel: adsorption equilibrium and kinetics, J. Hazard. Mater., 165 (2009) 52–62.
[17] A. Azizi, M.R. Alavi Moghaddam, M. Arami, Comparison of three treated pulp and paper sludges as adsorbents for RB19 dye removal, J. Residuals Sci. Technol., 8 (2011) 117–124.
[18] A. Azizi, M.R. Alavi Moghaddam, M. Arami, Removal of a reactive dye using ash of pulp and paper sludge, J. Residuals Sci. Technol., 9 (2012) 159–168.
[19] L. Liu, L. Kong, H. Wang, R. Niu, H. Shi, Effect of graphene oxide nanoplatelets on the thermal characteristics and shape-stabilized performance of poly (styrene-*co*-maleic anhydride)-*g*-octadecanol comb-like polymeric phase change materials, Sol. Energy Mater. Sol. Cells, 149 (2016) 40–48.
[20] M. Auta, B.H. Hameed, Coalesced chitosan activated carbon composite for batch and fixed-bed adsorption of cationic and anionic dyes, Colloids Surf., B, 105 (2013) 199–206.
[21] S. Chen, J. Hong, H. Yang, J. Yang, Adsorption of uranium (VI) from aqueous solution using a novel graphene oxide-activated carbon felt composite, J. Environ. Radioact., 126 (2013) 253–258.
[22] A. Umar, A.A. Naim, M.M. Sanagi, Synthesis and characterization of chitosan grafted with polystyrene using ammonium persulfate initiator, Mater. Lett., 124 (2014) 12–14.
[23] A.A. Naim, A. Umar, M.M. Sanagi, N. Basaruddin, Chemical modification of chitin by grafting with polystyrene using ammonium persulfate initiator, Carbohydr. Polym., 98 (2013) 1618–1623.
[24] V.K. Konaganti, R. Kota, S. Patil, G. Madras, Adsorption of anionic dyes on chitosan grafted poly (alkyl methacrylate)s, Chem. Eng. J., 158 (2010) 393–401.
[25] S.M. Yuen, C.C.M. Ma, Y.Y. Lin, H.C. Kuan, Preparation, morphology and properties of acid and amine modified multiwalled carbon nanotube/polyimide composite, Compos. Sci. Technol., 67 (2007) 2564–2573.
[26] C. Wang, J. Zhou, J. Ni, Y. Cheng, H. Li, Design and synthesis of pyrophosphate acid/graphene composites with wide stacked pores for methylene blue removal, Chem. Eng. J., 253 (2014) 130–137.
[27] A. Beheshti Ardakani, H.A. Panahi, A.H. Hasani, A.H. Javid, E. Moniri, Tin(IV) oxide nanoparticles grafted with *N*,*N*-dimethylacrylamide–allyl butyl ether for xylene adsorption, Int. J. Environ. Sci. Technol., 12 (2015) 1613–1624.

[28] X. Deng, L. Lü, H. Li, F. Luo, The adsorption properties of Pb(II) and Cd(II) on functionalized graphene prepared by electrolysis method, J. Hazard. Mater., 183 (2010) 923–930.
[29] S. Sheshmani, A. Ashori, S. Hasanzadeh, Removal of Acid Orange 7 from aqueous solution using magnetic graphene/chitosan: a promising nano-adsorbent, Int. J. Biol. Macromol., 68 (2014) 218–224.
[30] F. Su, C. Lu, S. Hu, Adsorption of benzene, toluene, ethylbenzene and *p*-xylene by NaOCl-oxidized carbon nanotubes, Colloids Surf., A, 353 (2010) 83–91.
[31] A. Azizi, M.R. Alavi Moghaddam, M. Arami, Application of response surface methodology for optimization of reactive blue 19 dye removal from aqueous solutions using pulp and paper sludge, Fresenius Environ. Bull., 20 (2011) 929–938.
[32] L. Wang, J. Zhang, R. Zhao, C. Li, Y. Li, C. Zhang, Adsorption of basic dyes on activated carbon prepared from *Polygonum orientale* Linn: equilibrium, kinetic and thermodynamic studies, Desalination, 254 (2010) 68–74.
[33] M. Aivalioti, P. Papoulias, A. Kousaiti, E. Gidarakos, Adsorption of BTEX, MTBE and TAME on natural and modified diatomite, J. Hazard. Mater., 207–208 (2012) 117–127.
[34] F. Yu, J. Ma, J. Wang, M. Zhang, J. Zheng, Magnetic iron oxide nanoparticles functionalized multi-walled carbon nanotubes for toluene, ethylbenzene and xylene removal from aqueous solution, Chemosphere, 146 (2016) 162–172.
[35] Z.Y. Sui, B.H. Han, Effect of surface chemistry and textural properties on carbon dioxide uptake in hydrothermally reduced graphene oxide, Carbon, 82 (2015) 590–598.
[36] L. Seifi, A. Torabian, H. Kazemian, G.N. Bidhendi, A.A. Azimi, A. Charkhi, Adsorption of petroleum monoaromatics from aqueous solutions using granulated surface modified natural nanozeolites: systematic study of equilibrium isotherms, Water Air Soil Pollut., 217 (2011) 611–625.
[37] H. Shakeri, M. Arshadi, J.W.L. Salvacion, Removal of BTEX by using a surfactant-bio originated composite, J. Colloid Interface Sci., 466 (2016) 186–197.
[38] A.A.M. Daifullah, B.S. Girgis, Impact of surface characteristics of activated carbon on adsorption of BTEX, Colloids Surf., A, 214 (2003) 181–193.
[39] C. Lu, F. Su, S. Hu, Surface modification of carbon nanotubes for enhancing BTEX adsorption from aqueous solutions, Appl. Surf. Sci., 254 (2008) 7035–7041.
[40] F. Yu, J. Ma, Y. Wu, Adsorption of toluene, ethylbenzene and m-xylene on multi-walled carbon nanotubes with different oxygen contents from aqueous solutions, J. Hazard. Mater., 192 (2011) 1370–1379.
[41] B. Bina, M.M. Amin, A. Rashidi, H. Pourzamani, Water and wastewater treatment from BTEX by carbon nanotubes and Nano-Fe, Water Resour., 41 (2014) 719–727.
[42] S.M. Koh, J.B. Dixon, Preparation and application of organo-minerals as sorbents of phenol, benzene and toluene, Appl. Clay Sci., 18 (2001) 111–122.
[43] N. Wibowo, L. Setyadhi, D. Wibowo, J. Setiawan, S. Ismadji, Adsorption of benzene and toluene from aqueous solutions onto activated carbon and its acid and heat treated forms: influence of surface chemistry on adsorption, J. Hazard. Mater., 146 (2007) 237–242.
[44] C.J.M. Chin, L.C. Shih, H.J. Tsai, T.K. Liu, Adsorption of *o*-xylene and *p*-xylene from water by SWCNTs, Carbon, 45 (2007) 1254–1260.
[45] W. Chen, L. Duan, D. Zhu, Adsorption of polar and nonpolar organic chemicals to carbon nanotubes, Environ. Sci. Technol., 41 (2007) 8295–8300.
[46] F. Yu, Y. Wu, X. Li, J. Ma, Kinetic and thermodynamic studies of toluene, ethylbenzene, and m-xylene adsorption from aqueous solutions onto KOH-activated multiwalled carbon nanotubes, J. Agric. Food Chem., 60 (2012) 12245–12253.
[47] C.P. Moura, C.B. Vidal, A.L. Barros, L.S. Costa, L.C.G. Vasconcellos, F.S. Dias, R.F. Nascimento, Adsorption of BTX (benzene, toluene, o-xylene, and p-xylene) from aqueous solutions by modified periodic mesoporous organosilica, J. Colloid Interface Sci., 363 (2011) 626–634.